Three-Dimensional Bright-Dark Soliton, Bright Soliton Pairs, and Rogue Wave of Coupled Nonlinear Schrödinger Equation with Time-Space Modulation

Junchao Chen and Biao Li

Nonlinear Science Center, Ningbo University, Ningbo 315211, P. R. China

Reprint requests to B. L.; E-mail: biaolee2000@yahoo.com.cn

Z. Naturforsch. **67a**, 483 – 490 (2012) / DOI: 10.5560/ZNA.2012-0045 Received December 2, 2011 / revised May 4, 2012

We systematically provide a similarity transformation reducing the (3+1)-dimensional inhomogeneous coupled nonlinear Schrödinger (CNLS) equation with variable coefficients and parabolic potential to the (1+1)-dimensional coupled nonlinear Schrödinger equation with constant coefficients. Based on the similarity transformation, we discuss the dynamics of the propagation of the three-dimensional bright–dark soliton, the interaction between two bright solitons, and the feature of the three-dimensional rogue wave with different parameters. The obtained results may raise the possibility of relative experiments and potential applications.

Key words: Coupled NLS Equation; Bright-Dark Soliton; Bright Soliton Pairs; Rogue Wave.

1. Introduction

In the past decade, there have been a great deal of theoretical and experimental investigations in models based on the coupled nonlinear Schrödinger (CNLS) or coupled Gross-Pitaevskii (CGP) equation [1-20], which can be used widely to describe many physical systems such as Langmuir and dispersive ion acoustic waves [21], nonlinearly coupled polarized plasma waves [22], coupled electromagnetic waves [23] in a dielectric, and for electric transmission lines [24] and so on. Moreover, the (1+1)-dimensional CNLS equation with varying coefficients have been investigated by means of different techniques in the literatures [25, 26]. For the higher-dimensional case, very recently, Kuetche et al. proved the complete integrability of the (2+1)-dimensional mixed CNLS equation (or modified Manakov model) by the Painlevé properties and the generalized Lax representation [27]. However, the realization of a higher-dimensional CNLS is still a challengeable topic for that adding a dimension may changes drastically the integrability properties of the equation. Only a few papers have paid attention to the (2+1)-dimensional situation [27-30] and the (3+1)-dimensional situation [31-35]. Therefore, we further focus on the (3+1)-dimensional CNLS equation with time- and space-dependent potential, timedependent nonlinearity, and gain or loss. Generally speaking, to obtain the corresponding analytical threedimensional soultion is still a difficult task. Fortunately, we may make use of the similarity transformation (see, e.g., [36] and references therein) to reduce the (3+1)-dimensional CNLS equation to the (1+1)dimensional one with constant coefficients, which allows us to use the solution of the complete integrable (1+1)-dimensional equation to construct the corresponding analytical solution for the variable coefficients' equation. Based on the similarity transformation, we present a detailed study on dynamics of three-dimensional bright-dark soliton and bright soliton pairs solutions of the (3+1)-dimensional CNLS equation. To our knowledge, few authors studied the soliton pairs solutions and their interaction properties for above model. In addition, the research of rogue waves is a new theme which attract more and more attention in the ocean [37], in wide aperture optical cavities [38], and in capillary wave experiments [39], nonlinear optics [40], and cigar-shaped Bose-Einstein condensates (BECs) [41]. So we also discuss the dynamics of three-dimensional rogue waves of the CNLS system.

The organization of the article is settled as follows. In Section 2, we derive the similarity transformation reducing the (3 + 1)-dimensional inhomoge-

neous CNLS equation with variable coefficients and parabolic potential to the (1+1)-dimensional CNLS equation with constant coefficients. In Section 3, we give the expressions of the bright–dark soliton, the bright soliton pairs, and rogue wavelike solutions. The propagation of the three-dimensional bright–dark soliton and the interaction between two bright solitons are investigated, and the dynamics of rogue wavelike solutions are also discussed. In Section 4, we give some conclusions of the paper. Finally, a similarity transformation for (3+1)-dimensional N-coupled NLS equations is given in the appendix.

2. The Similarity Transformation

The original three-dimensional variable coefficients inhomogeneous CNLS (VCNLS) equation with time–space modulation can be written in a dimensionless form [31–34] as

$$i\frac{\partial\Psi_{1}}{\partial t} = -\frac{1}{2}\nabla^{2}\Psi_{1} + V_{1}(\mathbf{r},t)\Psi_{1} + [G_{11}(t)|\Psi_{1}|^{2} + G_{12}(t)|\Psi_{2}|^{2}]\Psi_{1} + i\Gamma_{1}(t)\Psi_{1},$$

$$i\frac{\partial\Psi_{2}}{\partial t} = -\frac{1}{2}\nabla^{2}\Psi_{2} + V_{2}(\mathbf{r},t)\Psi_{2} + [G_{21}(t)|\Psi_{1}|^{2} + G_{22}(t)|\Psi_{2}|^{2}]\Psi_{2} + i\Gamma_{2}(t)\Psi_{2},$$
(1)

where the physical field $\Psi_j = \Psi_j(\mathbf{r},t)$ (j=1,2), $\mathbf{r} = (x,y,z) \in \mathbb{R}^3$, $\nabla \equiv (\partial_x,\partial_y,\partial_z)$ with $\partial_x = \partial/\partial_x$, the external potentials $V_j(\mathbf{r},t)$ (j=1,2) are real-valued functions of time and spatial coordinates, and the nonlinear coefficients $G_{ij}(t)$ (i,j=1,2) and gain or loss coefficients $\Gamma_j(t)$ (j=1,2) are real-valued functions of time.

Our first objective is to seek for a similar transformation connecting solutions of (1) with those of the (1+1)-dimensional CNLS equation with constant coefficients, i.e.,

$$\begin{split} &i\frac{\partial\Phi_{1}}{\partial\tau} + \frac{\partial^{2}\Phi_{1}}{\partial\xi^{2}} + 2\mu(|\Phi_{1}|^{2} + \delta|\Phi_{2}|^{2})\Phi_{1} = 0,\\ &i\frac{\partial\Phi_{2}}{\partial\tau} + \frac{\partial^{2}\Phi_{2}}{\partial\xi^{2}} + 2\mu(|\Phi_{1}|^{2} + \delta|\Phi_{2}|^{2})\Phi_{2} = 0. \end{split} \tag{2}$$

Here, the physical field Φ_j (j=1,2) are functions of two variables $\xi \equiv \xi(\mathbf{r},t)$ and $\tau \equiv \tau(t)$, which are to be determined in the following reduce procedure, and $\delta = \pm 1$, with the sign of the real constant μ ($|\mu|$ implies the strength of nonlinearity) represents focusing or defocusing Kerr nonlinearity in nonlinear optics theory, whereas, the attractive or repulsive interactions between the species in BEC theory. Equation (2)

is found to be completely integrable derived in the process of solving by the inverse scattering transform (IST) by Zakharov and Schulman (see [1] and references therein) and then through systematic analysis of the Painlevé integrability [2] for more general constant coefficients' CNLS equation. When $\delta = 1$, the aforementioned system (2) is a Manakov system [3], and bright and dark multisoliton solutions of the corresponding system have been derived with different procedures [3, 5-7]. In the pioneering works [42, 43], Afanasjev and Serkin analytically and numerically investigated the interaction of initially motionless solitons in a Manakov system and similar ones. At $\delta = 1$ for equal-amplitude orthogonal bright solitons, the interaction manifests itself as periodic inharmonic oscillations of the soliton polarization, while the soliton remains at the same time position. In birefringent fibres with linear eigenmodes the interaction of unequalamplitude bright solitons is suppressed and always finally repulsive. On the other case, $\delta = -1$, the aforementioned system (2) is called the mixed CNLS (or modified Manakov model), which has attracted a lot of attention recently. The known solutions (say as brightbright, bright-dark, dark-dark type one-soliton solutions) and some new solutions of the mixed CNLS equation have been unearthed [4, 7, 11] and then singular and nonsingular bright multisoliton solutions have been obtained in [12]. In order to control boundary conditions at infinity, we impose the natural constraints [44]

$$\xi \to 0 \ \ \text{at} \ \ r \to 0 \, , \ \ \xi \to \infty \ \ \text{at} \ \ r \to \infty \, .$$

We are looking for the solution of (1) in the form [44, 45]

$$\Psi_{1} = \rho_{1}(t) e^{i\varphi_{1}(\mathbf{r},t)} \Phi_{1}[\xi(\mathbf{r},t),\tau(t)],
\Psi_{2} = \rho_{2}(t) e^{i\varphi_{2}(\mathbf{r},t)} \Phi_{2}[\xi(\mathbf{r},t),\tau(t)],$$
(3)

with $\rho_i(t)$ and $\varphi_j(\mathbf{r},t)$ (j=1,2) being the real-valued functions of the indicated variables. Thus, we substitute transformation (3) with (2) into (1) and after relatively simple algebra analysis obtain the following system of partial differential equations:

$$2\tau_t - |\nabla \xi|^2 = 0, \ \xi_t + \nabla \xi \cdot \nabla \varphi_j = 0, \ \nabla^2 \xi = 0,$$
 (4)

$$\frac{1}{2}\rho_{j}\nabla^{2}\varphi_{j} + \rho_{jt} - \rho_{j}\Gamma_{j} = 0, \qquad (5)$$

$$|\nabla \varphi_j|^2 + 2\varphi_{jt} + 2V_j = 0, \ 2\mu \tau_t + \rho_j^2 G_{j1} = 0, 2\delta \mu \tau_t + \rho_j^2 G_{j2} = 0, \ (j = 1, 2).$$
 (6)

In conventional practice, if linear and nonlinear potentials are arbitrary given primarily, equations in system (4)–(6) are not compatible with each other. One, however, can pose the problem to find the functions $V_j(\mathbf{r},t)$, $G_{j1}(t)$, $G_{j2}(t)$, and $\Gamma_j(t)$ (j=1,2) such that system (4)–(6) becomes solvable. By solving (4), we can write the similarity variables $\xi(\mathbf{r},t)$, $\tau(t)$ and the phases $\varphi_j(\mathbf{r},t)$ (j=1,2) in the form

$$\xi(\mathbf{r},t) = \mathbf{c}(t) \cdot \mathbf{r} - \int_{0}^{t} \mathbf{c}(s) \cdot \mathbf{a}(s) ds,$$

$$\tau(t) = \frac{1}{2} \int_{0}^{t} |\mathbf{c}(s)|^{2} ds,$$

$$\varphi_{j}(\mathbf{r},t) = \mathbf{r}\Omega(t)\mathbf{r} + \mathbf{a}(t) \cdot \mathbf{r} + \omega_{j}(t),$$

$$j = 1, 2,$$
(7)

where $\mathbf{c}(t) = [c_x(t), c_y(t), c_z(t)], \ \mathbf{a}(t) = [a_x(t), a_y(t), a_z(t)], \ \Omega(t) = \mathrm{diag} \left[-\frac{\dot{c}_x(t)}{2c_x(t)}, -\frac{\dot{c}_y(t)}{2c_y(t)}, -\frac{\dot{c}_z(t)}{2c_z(t)} \right]$ (overdots stand for the derivative with respect to t), and $c_\sigma(t)$, $a_\sigma(t)$ ($\sigma = x, y, z$) and $w_j(t)$ (j = 1, 2) are functions of t. Then, from (5)–(6) we can derive the functions $G_j(t), V_j(\mathbf{r}, t)$, and $\rho_j(t)$ expressed by

$$G_{1}(t) \equiv G_{j1}(t) = -\frac{\mu |\mathbf{c}(t)|^{2} e^{-2 \int_{0}^{t} \Gamma_{1}(s) ds}}{\vartheta_{1}^{2} c_{x}(t) c_{y}(t) c_{z}(t)},$$

$$G_{2}(t) \equiv G_{j2}(t) = -\frac{\delta \mu |\mathbf{c}(t)|^{2} e^{-2 \int_{0}^{t} \Gamma_{2}(s) ds}}{\vartheta_{2}^{2} c_{x}(t) c_{y}(t) c_{z}(t)},$$

$$V_{i}(\mathbf{r}, t) = \mathbf{r} \Lambda(t) \mathbf{r} + \mathbf{b}(t) \cdot \mathbf{r} - \frac{1}{2} |\mathbf{a}(t)|^{2} - \dot{\boldsymbol{\omega}}_{j}(t),$$

$$\rho_{j}(t) = \vartheta_{j} \sqrt{c_{x}(t) c_{y}(t) c_{z}(t)} e^{\int_{0}^{t} \Gamma_{j}(s) ds}, \quad j = 1, 2,$$

where ϑ_1 and ϑ_2 are integration constants, $\Lambda(t) = \text{diag}[\alpha_x(t), \alpha_y(t), \alpha_z(t)]$, and $\mathbf{b}(t) = [b_x(t), b_y(t), b_z(t)]$ with

$$\alpha_{\sigma}(t) = \frac{\ddot{c}_{\sigma}(t)}{2c_{\sigma}(t)} - \frac{\dot{c}_{\sigma}^{2}(t)}{c_{\sigma}^{2}(t)},$$

$$b_{\sigma} = \frac{a_{\sigma}(t)\dot{c}_{\sigma}(t)}{c_{\sigma}(t)} - \dot{a}_{\sigma}(t), \ (\sigma = x, y, z).$$
(9)

Thus, from (8) – (9), we known that if $V_j(\mathbf{r},t)$ are linear potentials (first degree polynomial for x,y,z), then that $\alpha_{\sigma}(t)=0$, i.e., $\ddot{c}_{\sigma}(t)c_{\sigma}(t)-2\dot{c}_{\sigma}^2(t)=0$ must be hold, which denotes that $c_{\sigma}=c_1/(t+c_2)$. Correspondingly, if setting c_{σ} are other free functions of t except for the type of $c_1/(t+c_2)$, the parabolic potentials $V_j(\mathbf{r},t)$ (second degree polynomial for x,y,z) will be exhibited naturally. In what follows, we discuss the nontrivial dynamics of different three-dimensional solutions managed by (1) under the parabolic potentials.

3. Bright-Dark Soliton, Bright Soliton Pairs, and Rogue Wavelike Solutions

From the different parameter relations derived in Section 2, we can find that if choosing $c_{\sigma}(t)$, $a_{\sigma}(t)$ ($\sigma=x,y,z$), $\Gamma_j(t)$, $\omega_j(t)$, and ϑ_j (j=1,2), one can generate pairs $V_j(\mathbf{r},t)$ and $G_j(t)$ (j=1,2). Then the solutions of (1) can be obtained from those of (2) using (3). Meanwhile, one can note that for the given $c_{\sigma}(t)$ (or $\alpha_{\sigma}(t)$), the nonlinearities $G_j(t)$ must attenuate (grow) exponentially in the gain or loss medium $\Gamma_j(t)>0$ ($\Gamma_j(t)<0$), respectively. To make sure the frequencies $\alpha_{\sigma}(t)$ and nonlinearities $G_j(t)$ (j=1,2) are bounded for realistic cases, we choose $c_{\sigma}(t)$ and the gain or loss coefficients $\Gamma_j(t)$ (j=1,2) as the periodic functions

$$c_{\sigma}(t) = C_{\sigma}\operatorname{dn}(t, m_{\sigma}), \ a_{\sigma}(t) = 0, \ \sigma = x, y, z, \tag{10}$$

$$\Gamma_j(t) = \Upsilon_j \operatorname{cn}(\lambda_j t, n_j) \operatorname{dn}(\lambda_j t, n_j), \quad j = 1, 2, \tag{11}$$

where C_{σ} , Y_j , and λ_j are real constants, and $m_{\sigma} \in [0,1]$ and $n_1, n_2 \in [0,1]$ are the modules of Jacobi elliptic functions.

3.1. Bright-Dark Soliton

If simply setting $\mu = 1$ and $\delta = -1$, (2) becomes the mixed CNLS equation and the bright–dark soliton solutions of corresponding system can be expressed by the form [4, 11]

$$\Phi_{1} = p \operatorname{sech}\left[\sqrt{p^{2} + q^{2}}(\xi - k\tau)\right] e^{i(k\xi/2 - s_{1}\tau)},
\Phi_{2} = q \operatorname{tanh}\left[\sqrt{p^{2} + q^{2}}(\xi - k\tau)\right] e^{i(k\xi/2 - s_{2}\tau)},
s_{1} = \frac{k^{2}}{4} + (q^{2} - p^{2}), \quad s_{2} = \frac{k^{2}}{4} + 2q^{2},$$
(12)

where the real arbitrary parameter k denotes the velocity, and the real arbitrary parameters p and q represent the amplitudes of the components Φ_1 and Φ_2 , respectively.

The dynamics of the time-varying bright–dark soliton [in (3), (7)–(12)] at three different choices of the main managed parameters $c_{\sigma}(t)$ and $\Gamma_{j}(t)$ [in (10)–(11)] are illustrated in Figure 1. In Figure 1a, when $m_{\sigma}=0.1$, we can see that the frequencies $\alpha_{\sigma}(t)$ of potentials display periodicity distinctly, nonlinearities show $G_{1}(t)<0$ and $G_{2}(t)>0$ (for $\delta=-1$), and the bright–dark soliton propagates in a zigzag trace. When $m_{\sigma}=0.9$ ($m_{\sigma}\to 1$), Figure 1b show that the period and amplitude of $\alpha_{\sigma}(t)$ becomes bigger than results in Figure 1a, the amplitude of the bright soliton

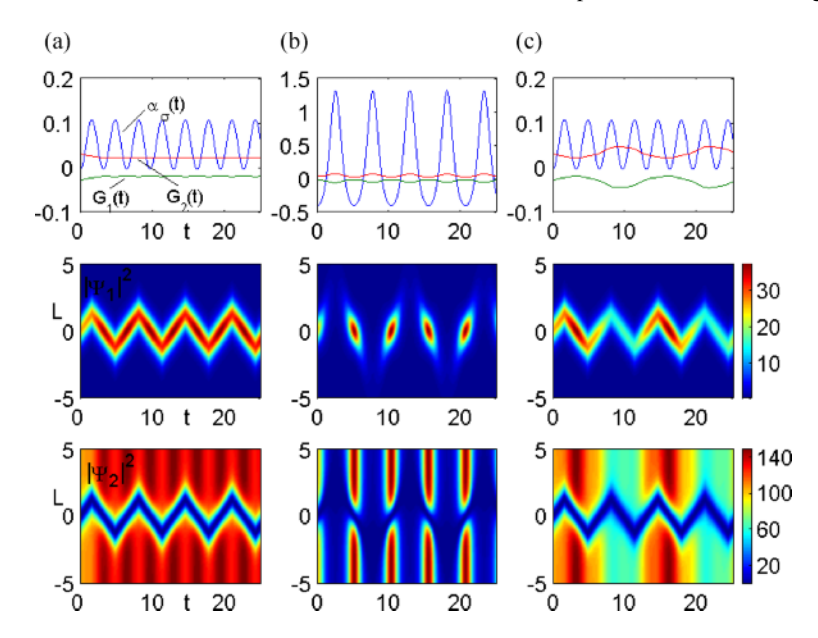


Fig. 1 (colour online). Density plots of $|\Psi_1|^2$ and $|\Psi_2|^2$ by (3), (7)–(12) with $L=C_xx+C_yy+C_zz$ and the parameters: (a) (left) $2k=2p=q=2\lambda_1=2\lambda_2=1$, $\vartheta_1=\vartheta_2=10$, $\varUpsilon_1=\varUpsilon_2=0.1$, $C_\sigma=1$, $n_1=n_2=1$, and $m_\sigma=0.1$; (b) (middle) $m_\sigma=0.9$ and the others are the same as (a); (c) (right) $n_1=n_2=0$ and the others are the same as (a).

close to the corners attenuates rapidly so that a soliton chain is generated, whereas, the relative amplitude of the dark soliton increases promptly to palisade-shape soliton emerge. It is also worthy to mention that for the case $m_{\sigma}=0$, one can easily find that $c_{\sigma}(t)=C_{\sigma}$ and $\alpha_{\sigma}(t)=0$, leading to zero external potential, in which the general travelling-wave soliton is obtained. In Figure 1c, if setting $n_{j}=0$, in which $G_{j}(t)$ change from a hyperbolic function to a trigonometric function, and the periodicities of them alter evidently, the amplitudes of the bright–dark soliton also yield the same periodic changes. For completeness, one can also select the bright–bright soliton solution, the dark–dark soliton solution or other type of solution to make some corresponding discussions [4, 7, 11, 12].

3.2. Bright Soliton Pairs

The interaction of the solitons plays an important role in the study of optics theory or BEC theory. Here, we only study the interaction between two bright solitons. If we set $\delta=1$, (2) is the integrable coupled NLS equation of Manakov type, and the corresponding two bright soliton solutions can read [7]

$$\Phi_1 = G/F, \ \Phi_2 = H/F,$$

$$G = \sum_{j=1}^2 s_j e^{\eta_j} + \sum_{j=1}^2 e^{\eta_1 + \eta_2 + \eta_j^* + \delta_j},$$

$$H = \sum_{j=1}^{2} h_{j} e^{\eta_{j}} + \sum_{j=1}^{2} e^{\eta_{1} + \eta_{2} + \eta_{j}^{*} + \Delta_{j}},$$

$$F = 1 + \sum_{j=1}^{2} e^{\eta_{j} + \eta_{j}^{*} + R_{j}} + e^{\eta_{1} + \eta_{2}^{*} + \delta_{0}}$$

$$+ e^{\eta_{1}^{*} + \eta_{2} + \delta_{0}^{*}} + e^{\eta_{1} + \eta_{2} + \eta_{1}^{*} + \eta_{2}^{*} + R_{3}}.$$
(13)

where

$$\begin{split} \mathbf{e}^{\delta_0} &= \frac{l_{12}}{k_1 + k_2^*}, \ \mathbf{e}^{\delta_1} &= \frac{(k_1 - k_2)(s_1 l_{21} - s_2 l_{11})}{(k_1 + k_1^*)(k_1^* + k_2)}, \\ \mathbf{e}^{\delta_2} &= \frac{(k_2 - k_1)(s_2 l_{12} - s_1 l_{22})}{(k_2 + k_2^*)(k_1 + k_2^*)}, \ \mathbf{e}^{R_1} &= \frac{l_{11}}{k_1 + k_1^*}, \\ \mathbf{e}^{R_2} &= \frac{l_{22}}{k_2 + k_2^*}, \ \mathbf{e}^{R_3} &= \frac{|k_1 - k_2|^2 (l_{11} l_{22} - l_{12} l_{21})}{(k_1 + k_1^*)(k_2 + k_2^*)|k_1 + k_2^*|^2}, \\ \mathbf{e}^{\Delta_1} &= \frac{(k_1 - k_2)(h_1 l_{21} - h_2 l_{11})}{(k_1 + k_1^*)(k_1^* + k_2)}, \end{split}$$

$$(14)$$

$$\mathbf{e}^{\Delta_2} &= \frac{(k_2 - k_1)(h_2 l_{12} - h_1 l_{22})}{(k_2 + k_2^*)(k_1 + k_2^*)}, \end{split}$$

and

$$l_{mn} = \frac{\mu(s_m s_n^* + h_m h_n^*)}{k_m + k_n^*}, \ \eta_j = k_j \xi + i k_j^2 \tau + \eta_j^{(0)}, \ (15)$$

with arbitrary complex parameters k_1 , k_2 , s_1 , s_2 , h_1 , h_2 , $\eta_1^{(0)}$, and $\eta_2^{(0)}$.

In Figure 2, the dynamics of the 3D time-varying bright two-soliton solutions are exhibited. We still give

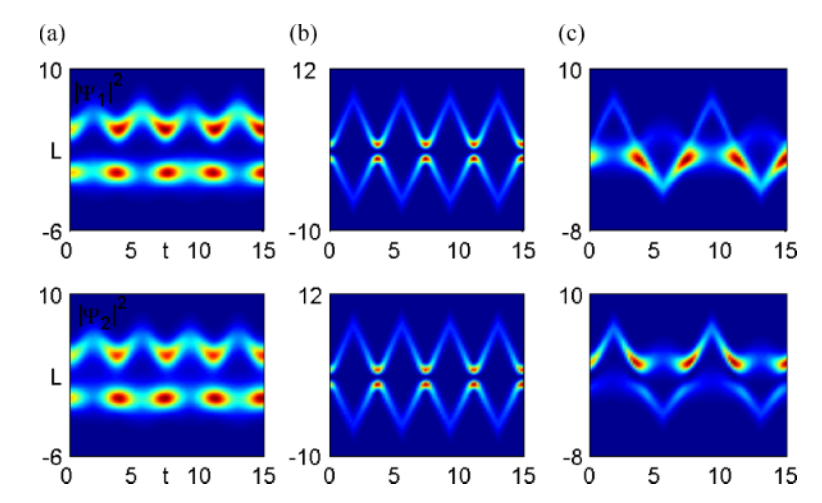


Fig. 2 (colour online). Density plots of $|\Psi_1|^2$ and $|\Psi_2|^2$ by (3), (7)–(11), and (13)–(15) with $L=C_xx+C_yy+C_zz$: (a) (left) $|\Psi_1|^2_{\max}=0.8264$ and $|\Psi_2|^2_{\max}=1.0129$ with the parameters: $\eta_1^{(0)}=\eta_2^{(0)}=0$, $\mu=\vartheta_1=\vartheta_2=s_1=s_2=h_1=k_1=2\lambda_1=2\lambda_2=1$, $Y_1=Y_2=0.1$, $C_\sigma=1$, $n_1=n_2=1$, $m_\sigma=0.5$, $k_2=1.2$, and $k_2=1+i$; (b) (middle) $|\Psi_1|^2_{\max}=1.6675$ and $|\Psi_2|^2_{\max}=1.6675$ with $k_2=1$, $k_1=1+i$, $k_2=1-i$ and the others are the same as (a); (c) (right) $|\Psi_1|^2_{\max}=1.1663$ and $|\Psi_2|^2_{\max}=2.3530$ with $k_2=i$, $k_2=1.2+0.6i$ and the others are the same as (a).

three different examples under different parameters but the fixed modules m_{σ} of Jacobi elliptic functions. Two strong zigzag solitons without interaction (see Fig. 2a), two strong zigzag solitons with interaction (see Fig. 2b), and strong-weak zigzag solitons with interaction (see Fig. 2c) can be classified mainly. In addition, similarly with Figure 1, if $m_{\sigma} \rightarrow 1$, the amplitudes of the soliton pairs close to the corners will almost decrease to zero so that the panel (a) will degenerate to two parallel soliton chains, whereas the panels (b) and (c) will degenerate to the ><-shaped soliton chains. Another same analysis, if the variation of $\Gamma_i(t)$ exist, the amplitudes of three soliton pairs will change followingly. Here, in the same way, one can also discuss the dynamic behaviour of other forms of soltion pairs such as two dark-dark soltions [7, 46] and two brightdark soltions [47] by the transformation in Section 2.

3.3. Rogue Wavelike Solutions

In this subsection, we make use of the rational solutions of the (1+1)-dimensional CNLS equation which serve as prototypes of rogue waves to illustrate the nontrivial dynamics of three-dimensional rogue wavelike solutions of VCNLS equation (1). First, we consider the first-order rational solution (one-rogon solution) of (2) which can be given $(\tau \to \frac{1}{2}\tau)$ by the form [49]

$$\begin{split} & \Phi_1 = \frac{sa}{\sqrt{2\mu(A^2 + B^2)}} \\ & \cdot \left[1 - \frac{(1 + 2is^2\tau)}{1 + 2s^2(\xi - 2k\tau)^2 + 4s^4\tau^2} \right] e^{i[k\xi + (s^2 - k^2)\tau]} \,, \end{split}$$

$$\Phi_{2} = \frac{sb}{\sqrt{2\mu(A^{2} + B^{2})}}$$

$$\cdot \left[1 - \frac{(1 + 2is^{2}\tau)}{1 + 2s^{2}(\xi - 2k\tau)^{2} + 4s^{4}\tau^{2}} \right] e^{i[k\xi + (s^{2} - k^{2})\tau]},$$
(16)

with arbitrary parameters s, μ , A, B, and k.

Then, when the second-order rational solution (two-rogon solution) of (2) is considered, the second-order rogue wave solutions of the VCNLS equation (1) can be derived immediately by the transformation (3). The second-order rational solution of (2) $(\tau \to \frac{1}{2}\tau)$ reads [49]

$$\begin{split} & \Phi_{1} = \frac{sa}{\sqrt{2\mu(A^{2} + B^{2})}} \\ & \cdot \left[1 + \frac{P(\xi, \tau) - is^{2}Q(\xi, \tau)}{H(\xi, \tau)} \right] e^{i[k\xi + (s^{2} - k^{2})\tau]}, \\ & \Phi_{2} = \frac{sb}{\sqrt{2\mu(A^{2} + B^{2})}} \\ & \cdot \left[1 + \frac{P(\xi, \tau) - is^{2}Q(\xi, \tau)}{H(\xi, \tau)} \right] e^{i[k\xi + (s^{2} - k^{2})\tau]}, \end{split}$$

with

$$P(\xi,\tau) = -\frac{s^4(\xi - 2k\tau)^4}{2} - 6s^6(\xi - 2k\tau)^2\tau^2$$

$$-10s^8\tau^4 - \frac{3s^2(\xi - 2k\tau)^2}{2} - 9s^4\tau^2 + \frac{3}{8},$$

$$Q(\xi,\tau) = s^4(\xi - 2k\tau)^4 + 4s^6(\xi - 2k\tau)^2\tau^2$$

$$+4s^8\tau^4 - 3s^2(\xi - 2k\tau)^2 + 2s^4\tau^2 - \frac{15}{4},$$

$$H(\xi,\tau) = \frac{s^6(\xi - 2k\tau)^6}{12} + \frac{s^8(\xi - 2k\tau)^4\tau^2}{2}$$
(18)

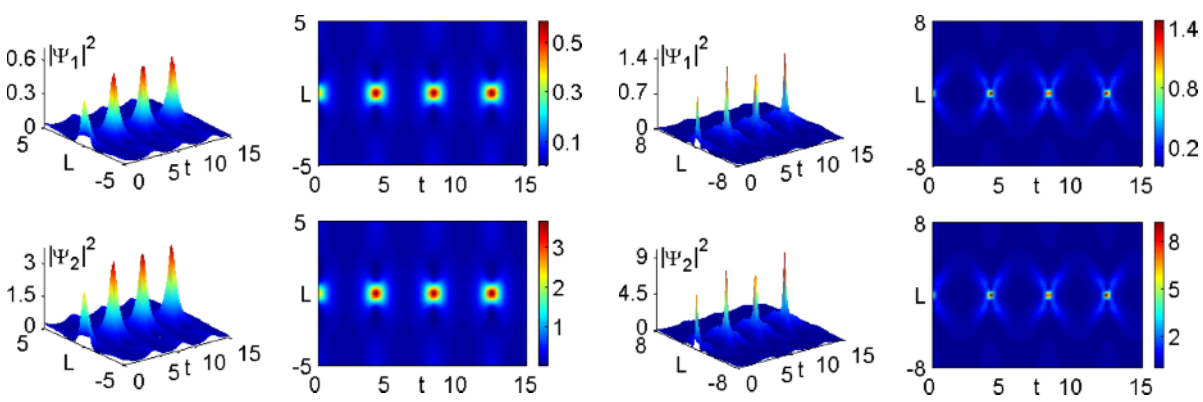


Fig. 3 (colour online). Intensity distribution (left) and density distribution (right) plots of $|\Psi_1|^2$ and $|\Psi_2|^2$ by (3), (7)–(11), and (16) with $L = C_x x + C_y y + C_z z$ and the parameters: $\mu = \vartheta_1 = \vartheta_2 = C_\sigma = n_1 = n_2 = 2\lambda_1 = 2\lambda_2 = 1$, $\Upsilon_1 = \Upsilon_2 = 0.1$, $m_\sigma = 0.7$, s = 0.8, A = 2, B = 5, and k = 0.

Fig. 5 (colour online). Intensity distribution (left) and density distribution (right) plots of $|\Psi_1|^2$ and $|\Psi_2|^2$ by (3), (7)–(11), and (17)–(23) with $L = C_x x + C_y y + C_z z$ and the parameters same as Figure 3.

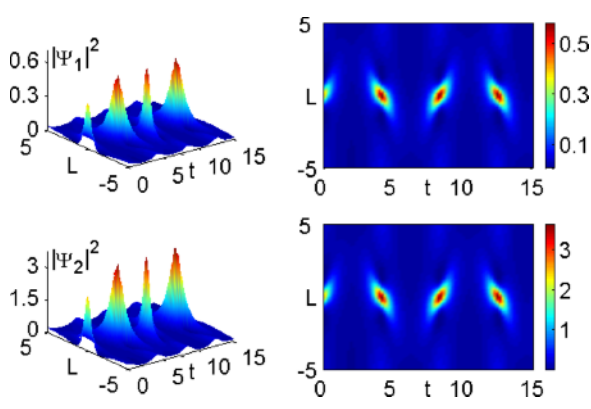


Fig. 4 (colour online). Intensity distribution (left) and density distribution (right) plots of $|\Psi_1|^2$ and $|\Psi_2|^2$ by (3), (7)–(11), and (16) with $L = C_x x + C_y y + C_z z$ and the parameters: k = 0.3 and the others are the same as Figure 3.

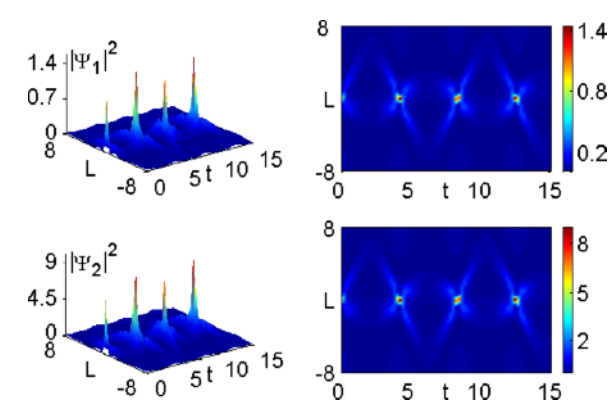


Fig. 6 (colour online). Intensity distribution (left) and density distribution (right) plots of $|\Psi_1|^2$ and $|\Psi_2|^2$ by (3), (7)–(11), and (17)–(23) with $L = C_x x + C_y y + C_z z$ and the parameters same as Figure 4.

$$\begin{split} &+\frac{2s^{12}\tau^6}{3}+s^{10}(\xi-2k\tau)^2\tau^4+\frac{s^4(\xi-2k\tau)^4}{8}\\ &+\frac{9s^8\tau^4}{2}-\frac{3s^6(\xi-2k\tau)^2\tau^2}{2}\\ &+\frac{9s^2(\xi-2k\tau)^2}{16}+\frac{33s^4\tau^2}{8}+\frac{3}{32}\,, \end{split}$$

with arbitrary parameters s, μ , A, B, and k.

From Figures 3-6, the dynamics of rogue wavelike solutions [(3), (7)-(11), and (16)-(23)] are depicted, which include the intensity distribution and density distribution plots of the first-order and second-order rogue wave solutions, respectively. As show in Figures 3 and 6, the rogue wave may be viewed as or-

derly arrangement along the t axis when setting k=0, but propagation in a zigzag trace along the t axis when $k=0.3 (k\neq 0)$. The features of these rogue wave solutions are localized in space and keep the localization infinitely in t-coordinate but differ from the usual rogue wave solutions [48]. Similarly with Figure 1, if $m_{\sigma} \rightarrow 1$, the width of the rogue wave will be diminished and if the variation of $\Gamma_j(t)$ exist, the amplitudes of previous wave will change [for (3) and (8c)], followingly.

4. Conclusions

In conclusion, we have presented a similarity transformation reducing the (3 + 1)-dimensional coupled

inhomogeneous nonlinear Schrödinger equation with variable coefficients to the (1+1)-dimensional one with constant coefficients. This transformation allows us to relate certain class of localized solutions of the (3+1)-dimensional case to the variety of solutions of integrable CNLS equation of the (1+1)dimensional case. As the application, we provide the specific expressions of the bright-dark soliton, the bright soliton pairs, and rogue wavelike solutions. At the same time, we focus on the bounded parabolic potential, nonlinearity, and gain or loss case to analyze the dynamics of the propagation of the threedimensional bright-dark soliton, the interaction between two bright solitons, and the feature of the threedimensional rogue wave with different parameters. The results can be applied to some physical fields, such as Bose-Einstein condensates, nonlinear optics, plasma physics, etc., and open up opportunities for further studies on relative experiments and potential applications.

Appendix: The Similarity Transformation for N-coupled NLS equation

In [50-52], the authors investigate the (1+1)-dimensional N-coupled NLS system from different view points. For example, Kanna and Sakkaravarthi [52] investigated the integrable N-component coherently coupled NLS equations describing simultaneous propagation of multiple fields in Kerr-type nonlinear media by a non-standard type of Hirota's bilinearization method, and the more general bright one solitons with single-hump and double-hump profiles including special flat-top profiles are obtained. So in this appendix, we will extend the results in the paper to three-dimensional N-coupled NLS equations and present the similarity transformations for them: for

$$i\frac{\partial \Psi_j}{\partial t} = -\frac{1}{2}\nabla^2 \Psi_j + V_j(\mathbf{r}, t)\Psi_j + \left[\sum_{k=1}^N G_k(t)|\Psi_k|^2\right]$$

$$\cdot \Psi_j + i\Gamma_j(t)\Psi_j, \quad (j = 1, 2, \dots, N)$$
(19)

we use the transformation

$$\Psi_i = \rho_i(t) e^{i\varphi_i(\mathbf{r},t)} \Phi_i[\xi(\mathbf{r},t), \tau(t)]$$
 (20)

and select the objective equation as

$$i\frac{\partial \Phi_j}{\partial t} + \frac{\partial^2 \Phi_j}{\partial^2 \xi} + 2\mu \left[\sum_{k=1}^N \delta_k |\Phi_k|^2 \right] \Phi_j = 0,$$

$$(j = 1, 2, \dots, N).$$
(21)

Then, the system of partial differential equations can be derived as

$$2\tau_{t} - |\nabla \xi|^{2} = 0, \quad \xi_{t} + \nabla \xi \cdot \nabla \varphi_{j} = 0,$$

$$\nabla^{2} \xi = 0, \quad \frac{1}{2} \rho_{j} \nabla^{2} \varphi_{j} + \rho_{jt} - \rho_{j} \Gamma_{j} = 0,$$

$$|\nabla \varphi_{j}|^{2} + 2\varphi_{jt} + 2V_{i} = 0, \quad 2\mu \delta_{j} \tau_{t} + \rho_{j}^{2} G_{j} = 0.$$
(22)

Solving these equations, the following results are obtained:

$$V_{j}(\mathbf{r},t) = \mathbf{r}\Lambda(t)\mathbf{r} + \mathbf{b}(t) \cdot \mathbf{r} - \frac{1}{2}|\mathbf{a}(t)|^{2} - \dot{\omega}_{j}(t),$$

$$\tau(t) = \frac{1}{2} \int_{0}^{t} |\mathbf{c}(s)|^{2} ds,$$

$$G_{j}(t) = -\frac{\delta_{j}\mu|\mathbf{c}(t)|^{2} e^{-2\int_{0}^{t} \Gamma_{j}(s) ds}}{\vartheta_{j}^{2} c_{x}(t) c_{y}(t) c_{z}(t)},$$

$$\rho_{j}(t) = \vartheta_{j} \sqrt{c_{x}(t) c_{y}(t) c_{z}(t)} e^{\int_{0}^{t} \Gamma_{j}(s) ds},$$

$$\xi(\mathbf{r},t) = \mathbf{c}(t) \cdot \mathbf{r} - \int_{0}^{t} \mathbf{c}(s) \cdot \mathbf{a}(s) ds,$$

$$\varphi_{j}(\mathbf{r},t) = \mathbf{r}\Omega(t)\mathbf{r} + \mathbf{a}(t) \cdot \mathbf{r} + \omega_{j}(t),$$
(23)

where $\Lambda(t) = \mathrm{diag}[\alpha_x(t), \alpha_y(t), \alpha_z(t)], \quad \Omega(t) = \mathrm{diag}[-\frac{\dot{c}_x(t)}{2c_x(t)}, -\frac{\dot{c}_y(t)}{2c_y(t)}, -\frac{\dot{c}_z(t)}{2c_z(t)}]$ (overdots stand for the derivative with respect to t), $\mathbf{a}(t) = [a_x(t), a_y(t), a_z(t)],$ $\mathbf{b}(t) = [b_x(t), b_y(t), b_z(t)], \quad \mathbf{c}(t) = [c_x(t), c_y(t), c_z(t)],$ $c_\sigma(t), \ a_\sigma(t) \ (\sigma = x, y, z), \text{ and } w_j(t) \ (j = 1, 2, \ldots, N)$ are functions of t; ϑ_1 and ϑ_2 are integration constants,

$$\alpha_{\sigma}(t) = \frac{\ddot{c}_{\sigma}(t)}{2c_{\sigma}(t)} - \frac{\dot{c}_{\sigma}^{2}(t)}{c_{\sigma}^{2}(t)},$$

$$b_{\sigma} = \frac{a_{\sigma}(t)\dot{c}_{\sigma}(t)}{c_{\sigma}(t)} - \dot{a}_{\sigma}(t).$$
(24)

Acknowledgement

This work is supported by Zhejiang Provincial Natural Science Foundations of China under Grant No. Y6090592, National Natural Science Foundation of China under Grant Nos. 11041003, Ningbo Natural Science Foundation under Grant Nos. 2010A610095, 2010A610103 and 2009B21003, and K. C. Wong Magna Fund in Ningbo University.

- E. V. Zakharov and E. I. Schulman, Physica D 4, 270 (1982).
- [2] R. Sahadevan, K. M. Tamizhmani, and M. Lakshmanan, J. Phys. A: Math. Gen. 19, 1783 (1986).
- [3] S. V. Manakov, Zh. Eksp. Teor. Fiz. 65, 505 (1973)[Sov. Phys. JETP 38, 248 (1974)].
- [4] V. G. Makhankov, N. V. Makhaldiani, and O. K. Pashaev, Phys. Lett. A 81, 161 (1981).
- [5] M. V. Tratnik and J. E. Sipe, Phys. Rev. A 38, 2011 (1988).
- [6] H. Sakaguchi and B. A. Malomed, Eur. Phys. Lett. 72, 698 (2005).
- [7] S. Rajendran, P. Muruganandam, and M. Lakshmanan, J. Phys. B 42, 145307 (2009).
- [8] S. Rajendran, M. Lakshmanan, and P. Muruganandam, J. Math. Phys. 52, 023515 (2011).
- [9] V. N. Serkin, A. Hasegawa, and T. L. Belyaeva, Phys. Rev. Lett. 98, 074102 (2007).
- [10] V. N. Serkin, A. Hasegawa, and T. L. Belyaeva, Phys. Rev. A 81, 023610 (2010).
- [11] E. N. Tsoy and N. Akhmediev, Opt. Commun. 266, 660 (2006).
- [12] T. Kanna, M. Lakshmanan, P. T. Dinda, and N. Akhmediev, Phys. Rev. E 73, 026604 (2006).
- [13] M. Li, B. Tian, W. J. Liu, Y. Jiang, and K. Sun, Eur. Phys. J. D 59, 279 (2010).
- [14] B. Li, X. F. Zhang, Y. Q. Li, Y. Chen, and W. M. Liu, Phys. Rev. A 78, 023608 (2008).
- [15] B. Li, F. Zhang, Y. Q. Li, and W. M. Liu, J. Phys. B: At. Mol. Opt. Phys. 44, 175301 (2011).
- [16] D. S. Wang, X. H. Hu, J. P. Hu, and W. M. Liu, Phys. Rev. A 81, 025604 (2010).
- [17] J. C. Chen and B. Li, Z. Naturforsch. 66a, 728 (2011).
- [18] X. J. Lai and X. O. Cai, Z. Naturforsch. 66a, 392
- [19] L. C. Liu, B. Tian, B. Qin, X. Lü, Z. Q. Lin, and W. J. Liu, Z. Naturforsch. 66a, 522 (2011).
- [20] V. V. Afanasjev, E. M. Dianov, and V. N. Serkin, IEEE J. Quantum Electron. 25, 2656 (1989).
- [21] B. K. Som, M. R. Gupa, and B. Dasgupta, Phys. Lett. A 72, 111 (1979).
- [22] Y. Inoue, Plasma Phys. 16, 439 (1976).
- [23] Y. Inoue, J. Phys. Soc. Jpn. 43, 243 (1977).
- [24] J. Yoshinaga, N. Sugimoto, and T. Kakutani, J. Phys. Soc. Jpn. 50, 2122 (1981).
- [25] D. Schumayer and B. Apagyi, Phys. Rev. A 69, 043620 (2004).
- [26] X. Y. Tang, Y. Gao, and P. K. Shukla, Eur. Phys. J. D 61, 677 (2011).
- [27] V. K. Kuetche, T. B. Bouetou, T. C. Kofane, A. B. Moubissi, and K. Porsezian, Phys. Rev. A 82, 053619 (2010).

- [28] M. Aguero, D. J. Frantzeskakis, and P. G. Kevrekidis, J. Phys. A: Math. Gen. 39, 7705 (2006).
- [29] M. Brtka, A. Gammal, and B. A. Malomed, Phys. Rev. A 82, 053610 (2010).
- [30] H. Q. Zhang, B. Tian, L. L. Li, and Y. S. Xue, Physica A 388, 9 (2009).
- [31] D. V. Skryabin and W. J. Firth, Phys. Rev. E **60**, 1019 (1999).
- [32] M. Modugno, D. Dalfovo, C. Fort, P. Maddaloni, and F. Minardi, Phys. Rev. A 62, 063607 (2000).
- [33] B. A. Malomed, H. E. Nistazakis, D. J. Frantzeskakis, and P. G. Kevrekidis, Phys. Rev. A 70, 043616 (2004).
- [34] V. A. Brazhnyi, and V. V. Konotop, Phys. Rev. E 72, 026616 (2005).
- [35] R. Navarro, R. Carretero-González, and P. G. Kevrekidis, Phys. Rev. A 80, 023613 (2009).
- [36] G. W. Bluman, A. Cheviakov, and S. Anco, Applications of Symmetry Methods to Partial Differential Equations, Springer, New York 2009.
- [37] A. R. Osborne, Nonlinear Ocean Waves, Academic, New York 2009.
- [38] A. Montina, U. Bortolozzo, S. Residori, and F. T. Arecchi, Phys. Rev. Lett. 103, 173901 (2009).
- [39] M. Shats, H. Punzmann, and H. Xia, Phys. Rev. Lett. 104, 104503 (2010).
- [40] Y. V. Bludov, V. V. Konotop, and N. Akhmebiev, Opt. Lett. 34, 3015 (2009).
- [41] Y. V. Bludov, V. V. Konotop, and N. Akhmediev, Phys. Rev. A 80, 033610 (2009).
- [42] V. V. Afanasjev and V. N. Serkin, Sov. Lightwave Commun. 3, 101 (1993).
- [43] V. V. Afanasjev and V. N. Serkin, Interaction of Vector Solitons, Nonlinear Guided Wave Phenomena, Vol. 15 of 1993 OSA Technical Digest Series, paper TuB13, Optical Society of America, Washington, DC 1993.
- [44] Z. Y. Yan and V. V. Konotop, Phys. Rev. E 80, 036607 (2009).
- [45] Z. Y. Yan, V. V. Konotop, and N. Akhmediev, Phys. Rev. E 82, 036610 (2010).
- [46] Y. Ohta, D. S. Wang, and J. K. Yang, Stud. Appl. Math. 127, 345 (2011).
- [47] M. Vijayajayanthi, T. Kanna, and M. Lakshmanan, Phys. Rev. A 77, 013820 (2008).
- [48] N. Akhmediev, A. Ankiewicz, and J. M. Soto-Crespo, Phys. Lett. A **373**, 2137 (2009).
- [49] Z. Y. Yan, Phys. Lett. A 375, 4274 (2011).
- [50] T. Xu, J. Li, H. Q. Zhang, Y. X. Zhang, W. Hu, Y. T. Gao, and B. Tian, Phys. Lett. A 372, 1990 (2008).
- [51] X. H. Meng, B. Tian, T. Xu, H. Q. Zhang, and Q. Feng, Physica A 388, 209 (2009).
- [52] T. Kanna and K. Sakkaravarthi, J. Phys. A: Math. Theor. 44, 285211 (2011).